Research Article J. Electrochem. Sci. Technol., 2017, 8(4), 282-293

Journal of Electrochemical Science and Technology
jecst.org

Simultaneous Voltammetric Determination of Mefenamic Acid and Paracetamol using Graphene Nanosheets/Nickel Oxide Nanoparticles Modified Carbon Paste Electrode

Ali Naeemy[1], Rozhina Gholam-Shahbazi[1,2], and Ali Mohammadi[1,3,*]

[1]*Pharmaceutical Quality Assurance Research Centre, Faculty of Pharmacy, Tehran University of Medical Sciences, P.O. Box 14155-6451, Tehran, Iran*

[2]*Faculty of Pharmacy, Pharmaceutical Sciences Branch, Islamic Azad University, Tehran - Iran (IAUPS)*

[3]*Nanotechnology Research Centre, Faculty of Pharmacy, Tehran University of Medical Sciences, P.O. Box 14155-6451, Tehran, Iran*

ABSTRACT

A new modified carbon paste electrode (CPE) was constructed based on nickel oxide nanoparticles (NiONPs) and graphene nanosheets (Gr) for simultaneous determination of paracetamol (PCM) and mefenamic acid (MFA) in aqueous media and pharmaceutical dosage forms. NiONPs were synthesized via a simple and inexpensive technique and characterized using X-ray diffraction method. Scanning electron microscopy was used for the characterization of the morphology of modified carbon paste electrode (NiONPs/Gr/CPE). Voltammetric studies suggest that the NiONPs and Gr provide a synergistic augmentation that can increase current responses by improvement of electron transfers of these compounds on the NiONPs/Gr/CPE surface. Using cyclic voltammetry, the NiONPs/Gr/CPE showed good sensitivity and selectivity for the determination of PCM and MFA in individually or mixture standard samples in the linear range of 0.1-30 μg mL^{-1}. The resulted limit of detection and limit of quantification were 20 and 60 ng mL^{-1} for PCM, 24 and 72 ng mL^{-1} for MFA, respectively. The analytical performance of the NiONPs/Gr/CPE was evaluated for the determination of PCM and MFA in pharmaceutical dosage forms with satisfactory results.

Keywords : Paracetamol, Mefenamic acid, Nickel oxide nanoparticles, Graphene nanosheets, Voltammetry

Received : 30 April 2017, Accepted : 23 September 2017

1. Introduction

Paracetamol (PCM, *N*-acetyl-*p*-aminophenol, acetaminophen, Fig. 1(a) [1], commonly known as an analgesic and an antipyretic medicine as is conventionally used. It acts as a painkiller by inhibiting prostaglandin's synthesis in the central nervous system and relieves fever by sedating the hypothalamic heat-regulating center PCM is clinically important, though the overdoses of PCM have been found to cause fatal hepatotoxicity and nephrotoxicity [2]. Mefenamic acid, (MFA, 2-[(2, 3-dimethylphenyl) amino] benzoic acid, Fig. 1(b) [1] is an important non-steroidal anti-inflammatory drug (NSAID) used to treat several pathologies. It is used to relieve the symptoms of many diseases such as rheumatoid arthritis, osteoarthritis, non-articular rheumatism, and sports injuries. Overdoses of MFA produce toxic metabolite accumulation that causes acute hepatic necrosis, inducing morbidity and mortality in humans. PCM and MFA are effective and analgesic agents used worldwide for the relief of mild to moderate pain associated with a headache, backache and rheumatoid arthritis. PCM is used for the reduction of fever of bacterial or viral origin. The combination of MFA with PCM is frequently prescribed as an analgesic and anti-inflammatory agent in rheumatoid arthritis [2,3].

*E-mail address: alimohammadi@tums.ac.ir

DOI: https://doi.org/10.5229/JECST.2017.8.4.282

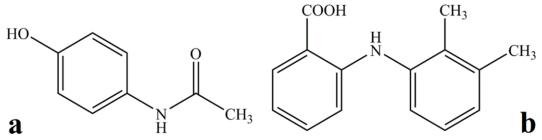

Fig. 1. The chemical structures of PCM (a) and MFA (b).

Accordingly, the determination of the levels of PCM and MFA present in pharmaceuticals is of considerable importance, to prevent overdoses leading to toxic effects. Different methods have been employed for the simultaneous determination of MFA with PCM in a pharmaceutical formulation which includes spectrophotometry [4-9], nuclear magnetic resonance spectroscopy [10], spectrofluorometry [11], high-performance liquid chromatography [12, 13], high-performance thin layer chromatography [14]. However, spectrophotometric and chromatographic methods usually require sample pretreatment (e.g. extraction, complex formation) which is laborious and time-consuming. To obviate these defects, electrochemical methods permit direct, simple and rapid determination without, in most instances, derivatization, requiring a minimum volume of the sample, is used for determination of a wide range of drugs in pharmaceutical preparations. Among electrochemical methods, modified electrodes are being used frequently in the voltammetric determination of organic and inorganic compounds because of their efficiency and the selectivity which the key factor in the construction of modified electrodes is to develop suitable modifier with catalytic activity, or conductivity, or absorbability [15,16].

Recently, a new kind of carbon material, graphene nanosheets (Gr), has attracted more attention in the field of modified electrodes. Gr – a one-atom-thick planar sheet of sp^2 bonded carbon atoms densely packed in a honeycomb crystal lattice is later discovered nanoscale form of carbon and has drawn immense attention in the fields of electronics, optical, magnetic, biological medicine, catalysis, and energy storage due to its special nanostructure and unique electronic properties [17,18]. It is reported that compared to single-walled carbon nanotubes, Gr exhibits 60 times more conductive, better sensitivity and stability, greater sp^2 character and also more surface negative charge density [19,20]. Hence it is now being widely used in sensor applications because of its large surface area, high electrocatalytic effect, rich edge defects and elevated mechanical strength [21]. It is an excellent 2D support to load polymers and other nanoparticles. The incorporation of such species effectively avoids the problem of aggregation of Gr arising from the Van der Waals interaction [22]. The achievement of high sensitivity, stability, selectivity, and low detection limit as well as wide linear range has been attributed to the extraordinary electron transport property and high electrocatalytic activity of Gr and the unique 2D crystal structure of Gr which serve as the substrate support for metal or metal-oxide catalyst nanoparticles [23,24].

In the past decades, there has been considerable attention to the synthesis of metal nanostructures due to their different physical and chemical properties related to their similar large-scale ones, and potential applications in optical, electronic, catalytic and magnetic devices [27-29]. Especially, combine unique properties of Gr and catalytic properties of metal nanoparticles, provided various applications as electrocatalysts, sensors and so on [29-31]. In recent years, the preparation of metal nanoparticles and their applications have received greater attention in materials science, owing to their catalytic properties and electrical conductivities, such as platinum, palladium, silver and gold. They can be used to promote electron transfer reactions when used as electrode materials in electrochemical devices [3,4]. Among the metal nanostructures, nickel oxide nanoparticles (NiONPs) has attracted much attention for development of modified electrodes due to their cost effectiveness, high electrocatalytic effect, biocompatibility, non-toxicity and high chemical stability [25,26]. Hitherto, there are no reports on NiONPs/Gr for the simultaneous determination of PCM and MFA. Therefore, we aim to exploit the synergistic effect of the catalytic activity of NiONP; together with the high conductivity and surface area of Gr to serve as a potential electrode material for the simultaneous determination of PCM and MFA.

The current paper presents for the first time, the use of a NiONPs/Gr modified carbon paste electrode (NiONPs/Gr/CPE) as a highly sensitive sensor for the simultaneous detection of PCM and MFA. Excellent reproducibility, low detection limits and good recovery values attained for commercial pharmaceutical tablets analysis, exhibit the reliability of the modified sensor.

2. Experimental

2.1. Chemical and reagents

PCM (99.94%) and MFA (98.66%) as working

standard powders were obtained from the Iranian Quality Control Laboratory of the Ministry of Health and Medical Education Department in Iran. Except for Gr, all chemicals used were of analytical grade (Merck, Darmstadt, Germany) and were used without further purification. Gr (purity> 99.5%, diameter 5-10 μm, layers <30 μm, thickness of 4-20 nm and a volume resistivity of 4×10^{-4} ohm cm) was prepared from Nanostructured & Amorphous Materials (USA). Pharmaceutical formulations of PCM and MFA were purchased from the local pharmacies. All voltammetric investigations were performed in deoxygenated solutions by purging the pure argon (99.999%, Roham Gas Company, Iran). Deionized water was used for all aqueous solution preparations.

2.2. Instrumentation

Electrochemical experiments were performed using an electrochemical system comprising of PC controlled μ-AUTOLAB TYPE III potentiostat/galvanostat with NOVA 1.11 electrochemistry software (ECO-Chemie, Utrecht, The Netherlands). The three-electrode cell system consisted of a CPE revealing a geometric surface area of 0.0314 cm^2, a platinum (Pt) rod and a dual Ag/AgCl, 3 mol L^{-1} KCl (Metrohm, Switzerland) [+0.197 V vs. SHE] were used as working, counter and reference electrodes, respectively. The x-ray diffraction (XRD) pattern was measured by a "Philips X'pert", using Cu Kα radiation at 40 kV and 30 mA. The surface morphology of modified electrode was determined using field emission scanning electron microscopy (FE–SEM, S-4160, Hitachi, Japan). All measurements were taken at room temperature of 25 ± 2ºC.

2.3. Preparation of stock and standard solutions

The stock solutions of PCM and MFA were freshly prepared by dissolving an accurate mass of their powders in an appropriate volume of deionized water (0.2 mg mL^{-1}). These solutions were protected from light using aluminium foil and stored at 4ºC for 2 days without any decomposition. Standard solutions were prepared daily by accurate dilution of PCM and MFA stock solutions by 0.1 M NaOH (which was also used as supporting electrolyte) for obtaining solutions with final concentrations of 0.1, 5, 10, 15, 20, 25 and 30 μg mL^{-1}, just before use.

2.4. Preparation of NiONPs

NiONPs nanoparticles were synthesized via a simple and inexpensive technique. Analytical grade nickel (II) nitrate was used as a metal precursor. In a typical synthesis, nickel nitrate and citric acid (molar ratio 2: 1) were dissolved in 250 mL of deionized water with magnetic stirring at room temperature to form a homogeneous solution. Ammonia solution (25%) was added dropwise to adjust the pH to 7. The prepared sol was placed in a water bath at 70ºC for 2 h under uniform stirring with a magnetic stirrer. After this time, the sol loses water gradually, and eventually, viscous gel remains. This gel precursor is preheated for further dehydration, which is followed by a sudden self-combustion, resulting in the evolution of large amounts of gasses. Flames extinguish within a few seconds, while the smoldering has appeared for several minutes, which results in the formation of fluffy foam. After the reaction, the powder was cooled to room temperature and then calcinated at 400ºC for 2 h. The calcined product was then pulverized, used for characterization and kept in the dark for preparing modified CPE.

2.5. Electrode preparation

In this work, all electrochemical studies were done using NiONPs/Gr/CPE and compared with the electrochemical responses of different electrodes including CPE, Gr/CPE, NiONPs/CPE, Ni microparticles/Gr/CPE (NiMPs/Gr/CPE) and Ni rod.

At first, CPE was prepared by hand-mixing carbon powder (60 mg) and paraffin (10.4 mg). The paste was carefully mixed and homogenized in an agate mortar for 10 mins and was kept at room temperature in a desiccator before use. The paste was packed firmly into a cavity (3.0 mm diameter) at the end of a teflon tube.

The Gr/CPE and NiONPs/CPE were prepared by mixing carbon powder together with NiONPs and Gr, respectively, with a 1:1 (w/w) ratio and an appropriate amount of paraffin (10.4 mg) in an agate mortar until a uniform paste was obtained. The electrode surface was gently smoothed by rubbing on a clean glass just prior to use. The NiONPs/Gr/CPE was prepared by mixing carbon powder together with NiONPs and Gr at different ratios in an agate mortar until a uniform paste was obtained. The percentage (w/w) of NiONPs, Gr and carbon powder informed throughout the text corresponds to the final percent-

age relative to the total paste composition. The percentage relative of 1:2:3 (carbon powder: Gr: NiONPs, w/w) used for paste preparation and packed into the cavity at the end of a Teflon tube and the electrical contact was established via a silver wire connected to the paste in the inner hole of the tube. The NiMPs/Gr/CPE was prepared same as the NiONPs/Gr/CPE with the difference using Ni microparticles (purchased from Neutrino Co., Iran) instance of NiONPs.

Cylindrical Ni rod of 99.9% purity was sealed with teflon to obtain the polycrystalline Ni working electrode (Ni rod). The Ni rod surface was polished with sandpaper and 0.05 mm alumina powder to the mirror finish and was subsequently rinsed with deionized water.

2.6. Determination of electroactive surface area

The electroactive surface area of the NiONPs/Gr/CPE was determined after each modification step and before applying for the determination of the PCM and MFA. The electrochemical probe molecules, $[Fe(CN)_6]^{3-}$/$[Fe(CN)_6]^{4-}$ were chosen to characterize the NiONPs/Gr/CPE. The electroactive surface area of the NiONPs/Gr/CPE was determined using 1 mM $K_4Fe(CN)_6$ in 0.1 M KCl electrolyte by recording the cyclic voltammograms (CVs). From the CVs anodic peak currents (I_{pa}) and the diffusion coefficient (D_o) of hexacyanoferrate, the electroactive surface area of the NiONPs/Gr/CPE was calculated according to the equation [27, 28]:

$$I_{pa} = (2.69 \times 10^5) n^{3/2} A D_0^{1/2} v^{1/2} C_0^* \quad (1)$$

where n is a number of electrons transferred, i.e., in this case, 1, A is the surface area of the electrode, D_o is the diffusion coefficient (2.4×10^{-6} cm^2 s^{-1}), v = scan rate (0.1 V s^{-1}), C_0^* is concentration of electroactive species (1 mM). The surface area of the NiONPs/Gr/CPE was estimated to be about 8 times of Ni rod.

2.7. Preparation of pharmaceutical dosage forms

For the analysis of PCM in tablets, twenty PCM 500 mg tablets were weighed and finely powdered and mixed. An amount of powder equal to the weight of one tablet containing 500 mg of PCM was accurately weighed and transferred to a 1000 mL volumetric flask and half filled with deionized water. After the solution was sonicated for 40 min, again diluted by deionized water and adjusted to the volume. Then, the solution was filtered through a 0.45 μm nylon filter (Chrom Tech, Apple Valley, MN, USA) and finally, 8 mL of filtered solution transferred to the 20 mL volumetric flask and diluted with 0.1 M NaOH to reach the target concentration (200 μg mL^{-1}) and transferred to the electrochemical cell for measurement.

For the analysis of the MFA in capsules, twenty MFA 250 mg capsules opened and the powder inside them individually were weighted and mixed fine. A fractional of powder equivalent to the content weight of one capsule containing 250 mg of the MFA was dissolved in 1000 mL volumetric flask and half filled with deionized water. It was sonicated for 20 min to affect complete dissolution and then made up to volume with deionized water. Then, the solution was filtered, diluted with 0.1 M NaOH to reach the target concentration (200 μg mL^{-1}) and transferred to the electrochemical cell for measurement.

3. Results and Discussion

3.1. Characterization of the NiONPs/Gr/CPE

3.1.1. FE-SEM Observation

The surface morphologies of the Gr and the NiONPs/Gr/CPE were examined by FE-SEM images. Fig. 2 shows the FE-SEM micrographs of Gr (A) and the NiONPs/Gr/CPE (B). Paper-like structure with a few micrometers dimensions is observed in the micrograph of Gr. On the other hand, NiONPs are homogeneously dispersed on the paste as small nanoparticles (dots) with an average diameter of ≤ 50 nm.

3.1.2. XRD analysis

X-ray diffraction pattern of NiONPs is shown in Fig. 3. The characteristic peaks are centered at 2θ values of ca. 37.30°, 43.41°, 63.03°, 75.65° and 79.47° which are correspond to the planes of (111), (200), (220), (311) and (222), respectively. Accordingly, the product is cubic NiO phase crystalline (Joint Committee on Powder Diffraction Standards (JCPDS) file No. 47-1049), and additional diffraction peaks of Ni are also found (JCPDS No. 04-0850). From a peak at 2θ = 43.41° with Miller indices (200) we have estimated the crystallite size d of the samples using Scherrer equation [29]:

$$d = 0.9\lambda / \beta \cos\theta \quad (1)$$

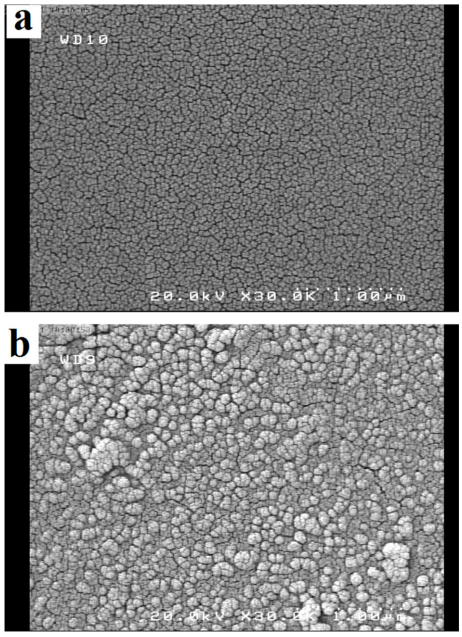

Fig. 2. SEM photographs of Gr (a) and NiONPs/Gr/CPE (b).

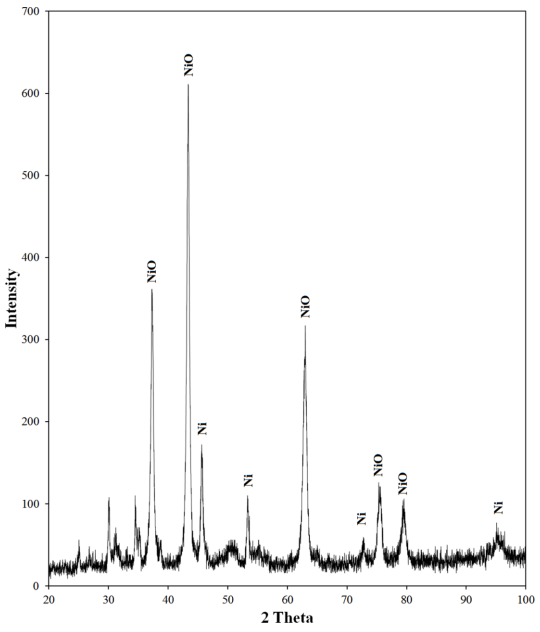

Fig. 3. The XRD patterns of NiO nanoparticles prepared by the sol-gel method.

where d is the grain diameter, β is the half-intensity width of the relevant diffraction, λ is X-ray wavelength and θ is the diffraction angle. The lattice parameter was calculated according to the following equation:

$$a = d_{hkl} (h^2 + k^2 + l^2)^{0.5} \quad (2)$$

Variables h, k, and l are called Miller indices and are the reciprocals of intersection distances of the lattice planes, d is interplanar distance and a is the unit cell length. The reflection plan (200) was used to calculate the crystallite size and lattice constant since this crystallographic plane exhibited the maximum diffraction intensity. The lattice parameter estimated from the strongest diffraction peak of (200) is 9.26 Å. This value is close to the known of bulk NiONPs [30]. The average crystallite size of the resulting NiONPs was 25 nm.

According to Fig. 3, the sharp diffraction peaks indicate good crystallinity of the nanocrystals. Further, the XRD pattern consists of fairly broad but still resolved peaks superimposed on a smoothly varying intensity. There are no other detectable traces of extra crystalline or amorphous phases. The considerable broadening of all diffraction peaks, amounting up to 1° full width at half maximum for the strongest peaks at 43.41° phase (200) indicates that the investigated samples consist of highly crystalline particles and quite small crystallites in size. These results match well with the previous report [28]. The presence of strains and stacking faults can also be exempted [29].

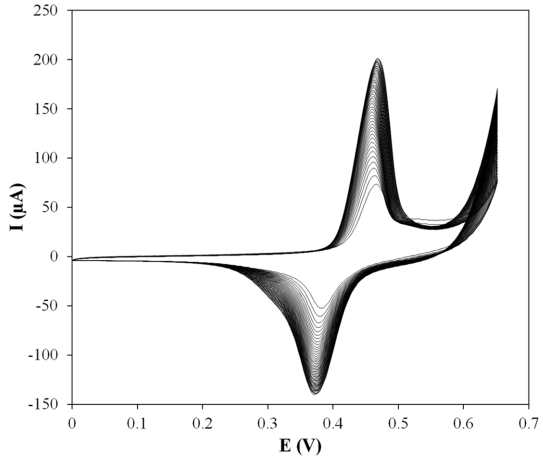

Fig. 4. Consecutive cyclic voltammograms of NiONPs/Gr/CPE oxidation in 0.1 M NaOH at a potential scan rate of 0.1 V s^{-1}.

3.2. Electrochemical behaviour of NiONPs/Gr/CPE.

Fig. 4 presents consecutive CVs of a NiONPs/Gr/CPE in 0.1 M NaOH solution recorded at a potential scan rate of 0.1 V s^{-1}. In the first scan, a pair of redox peaks appears at 0.51 and 0.39 V is assigned to Ni(II) / Ni(III) redox couple in alkaline media. In the subsequent cycles, the peaks shift cathodically and stabilize at 0.491 and 0.378 V, respectively. The entire behaviour is in accord with the data reported previously in the literature concerning the formation and interconversion of α and β-phases of $Ni(OH)_2$, its conversion to NiOOH and the enrichment of Ni(III) species on or just beneath the surface.

3.3. Electrochemical behavior of PCM and MFA

Cyclic voltammetric studies of 20 μg mL^{-1} of PCM and MFA in 0.1 M NaOH solution were done at the surfaces of CPE, Ni rod, Gr/CPE, NiONPs/CPE, NiMPs/Gr/CPE and NiONPs/Gr/CPE at a scan rate of 0.1 V s^{-1}. As can be seen in Fig. 5A, CPE and Gr/CPE in the presence of 20 μg mL^{-1} of PCM in 0.1 M NaOH solution had no electrochemical response and only baseline were observed (Fig. 5A, curves b and c). On the NiONPs/Gr/CPE, a higher peak current of the catalytic oxidation of 20 μg mL^{-1} of PCM compared to the Ni rod, NiONPs/CPE and NiMPs/Gr/CPE in 0.1 M NaOH solution observed (Fig. 5A, curves d-g), which is caused nanosize effect of NiONPs and high active surface area due to presence of Gr as well as the concentration β-NiOOH is more surface form. β-NiOOH is an electroactive form for oxidation of PCM, but the form γ-NiOOH appeared to be inactive and can be considered as species electro passive in the process [31]. As mentioned, this phase under successive cycles and rapid charge/discharge occurs. With the removal of hydrogen atoms or protons during charging, the repulsion between NiONPs to increase the space between the layer and the nickel film increases, the water, and metal ions stay between the layers of NiONPs. The space between the lower layers, the inter-electrode resistance is lower and thus better efficiency is obtained [32]. Maksimovic and Brunel [33] reported that due to the adsorption of oxygen on the nickel rod, oxidation current measurement is difficult on it. Dissolved molecular oxygen in the solution adsorbed to Ni rod surface and the reaction prevents. However, for NiONPs/Gr/CPE catalytic activity was observed. More of the response of NiONPs/Gr/CPE (Fig. 5A, curve g) rather than NiMPs/Gr/CPE (Fig. 5A, curve f) shows that the impact of nano-sized nickel and lattice constant slowly increases. Network expansion and empty d orbital less led to the exclusion of oxygen adsorption on the NiONPs/Gr/CPE surface and also increases the catalytic activity of NiONPs/Gr/CPE. Comparison of the CVs of NiONPs/Gr/CPE and NiONPs/CPE (Fig. 5A, curves g and e, respectively) also shows that response of NiONPs/Gr/CPE is higher than the NiONPs/CPE. In fact, Gr with their large surface area increase the adsorptive sites, resulting in a significant increase in the oxidation peak cur-

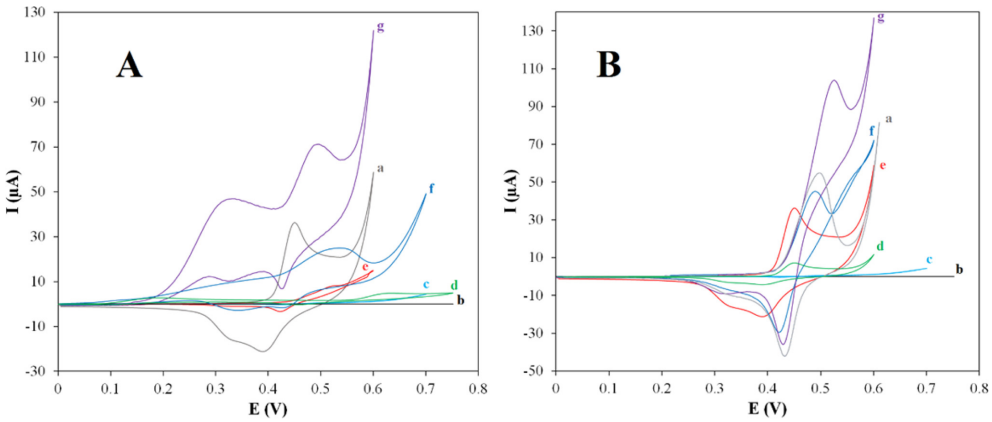

Fig. 5. Cyclic voltammograms for 20 μg mL^{-1} of (A) PCM and (B) MFA in 0.1 M NaOH solution on the surface of various electrodes; curve (a) NiONPs/Gr/CPE in the absence of analytes, (b) CPE, (c) Gr/CPE, (d) Ni rod, (e) NiONPs/CPE, (f) NiMPs/Gr/CPE and (g) NiONPs/Gr/CPE in the presence of analytes (Error bars show standard deviation of triplicate measurements). The potential scan rate was 0.1 V s^{-1}.

rent. Its mean that, in the presence of Gr nanosheets for the NiONPs/Gr/CPE related to NiONPs/CPE, the electrochemical responses toward drugs are enhanced, resulting from the high density of edge plane-like defective sites and oxygen containing functionalized group (depend on the reduction extent) on Gr providing more active sites that are beneficial for accelerating electron transfer between the electrode and drug species in solution. Additionally, π-π stacking interactions between drug and rich conjugated-structure of Gr resulting in capability to strongly adsorb target species enhance the surface concentration and greatly improve the sensitivity of PCM and MFA determination [23,34].

According to Fig. 5A, in the presence of PCM an additional anodic peak around 0.29 V on the electrode surface also appeared. To investigate the nature of this anodic peak, cyclic voltammograms using a NiONPs/Gr/CPE in 0.1 M NaOH solution in the absence and presence of PCM were recorded, and are shown in the Fig. 5A, curves a and g, respectively. In the absence of PCM, an anodic peak appeared at around 0.48 V which is attributable to the Ni^{+2}/ Ni^{+3} redox transition. In the presence of PCM, an additional anodic peak which is more negative than the Ni^{+2}/ Ni^{+3} redox transition appeared in two distinct areas (the potential of 0.19-0.4 V and 0.41-0.55 V). The first anodic peak of catalytic oxidation of PCM is that Ni^{+3} takes through the chemical reduction potential regenerating Ni^{+2} during the scan. The appearance of this anodic peak indicates that PCM oxidation prior to oxidation of $Ni(OH)_2$ to NiOOH is done [35,36]. In other words, there is a separation between the peak oxidation of $Ni(OH)_2$/NiOOH and catalytic oxidation peak of PCM and its demonstrated rapid kinetic of catalytic reaction between PCM and NiOOH in comparison with the redox reaction of adsorbed $Ni(OH)_2$/NiOOH [35-38]. Also, in the CV of NiONPs/Gr/CPE in the presence of PCM (Fig. 5A (g)), the peak potential of Ni (III) electrooxidation shifted toward more positive values (0.53 V) compared to the absence of PCM (0.48 V, Fig. 5A (a)). This indicates the interaction of PCM with the NiONPs/Gr/CPE surface is created. PCM molecules adsorbed on the surface are oxidized in the potential of 0.29 V before to the oxidation of Ni (II) to Ni (III) species at higher potentials which the presence of intermediates and products of the PCM oxidation at the surface. Along this line, Ni (II) species required the passage of the surface resistance due to presence of intermediates and products for the regeneration of Ni (III) as a result of the anodic pick potential shifted to more positive values (0.48 V to 0.53 V).

In Fig. 5B, cyclic voltammograms of 20 μg mL^{-1} of MFA in 0.1 M NaOH solution were done at the surfaces of CPE, Ni rod, Gr/CPE, NiONPs/CPE, NiMPs/Gr/CPE and NiONPs/Gr/CPE at a scan rate of 0.1 V s^{-1}. In the case of MFA oxidation mechanism, we can be seen in Fig. 5B, anodic peak increased in the potential 0.48 V in the presence of MFA and oxidation peak potential of Ni^{+2}, from 0.48 V is passing to more positive value of 0.53 V. In fact, this indicates that a strong interaction between MFA and the surface of electrode is created. MFA oxidation continues in reverse cathodic scan that it indicates the exodus of desorption intermediate and products, and regeneration of the surface adsorption active sites for MFA. It was observed that the anodic current and the associated anodic charge increased drastically, while the cathodic current and the corresponding charge decreased. In the presence of MFA, the anodic charge associated with the anodic peak is quantitatively 96.43% that of the corresponding cathodic peak, while in the absence of MFA it is 12.17%. This result indicates that MFA is oxidized by active nickel moiety through a cyclic mediation redox process. Nickel species are immobilized on the electrode surface, and the one with a higher valence oxidizes MFA via a chemical reaction followed by generation of low-valence nickel. Along this line, the high-valence oxide is regenerated through the external electrical circuit. Accordingly, MFA is also oxidized via an EC mechanism. Moreover, the significant current in the reverse sweep indicates that the reaction of MFA with high-valence nickel oxide is the rate-determining step of the oxidation process.

Based on the reported results, the following mechanism can be proposed for the mediated oxidation of the drugs on the modified surface. The corresponding kinetics is also formulated. The redox transition of the nickel species,

$$Ni^{2+} \leftrightarrow Ni^{3+} + e \quad (3)$$

is followed by the oxidation of drugs on the modified surface via the following reaction:

$$Ni^{3+} + drug \rightarrow product + Ni^{2+} \quad (4)$$

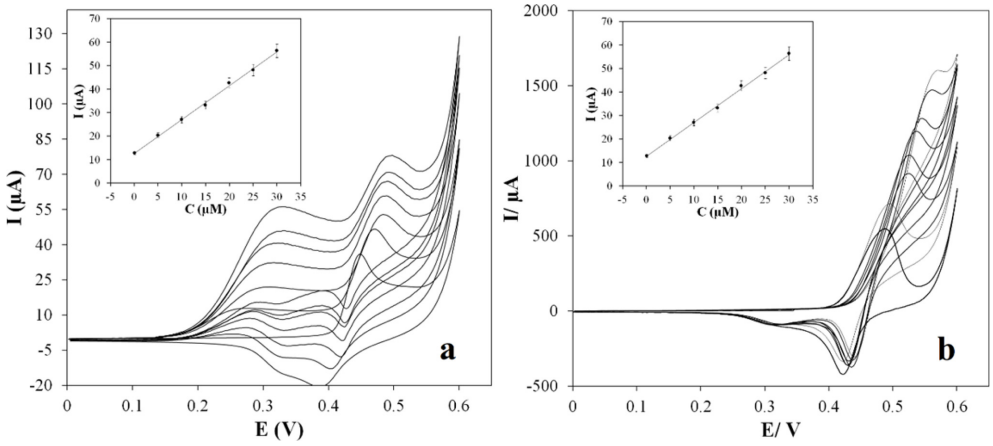

Fig. 6. Main panel: Cyclic voltammograms of various concentrations of (a) PCM and (b) MFA (down to up: 0, 0.1, 5, 10, 15, 20, 25 and 30 μg mL^{-1}) at NiONPs/Gr/CPE in 0.1 M NaOH solution. The potential scan rate was 0.1 V s^{-1}. Inset: Dependency of the charge under the anodic peak on the concentration of each one in solution.

Table 1. Characteristics of the calibration curves of the cyclic voltammetric determinations of PCM and MFA in 0.1 M NaOH solution.

Drug	Linear range (μg mL^{-1})	Linear Equation	Correlation coefficient (R^2)	LOQ (ng mL^{-1})	LOD (ng mL^{-1})
PCM[a]	0.1-30	y = 1.4462x + 12.644	0.995	60	20
MFA[a]	0.1-30	y = 2.7741x+ 62.925	0.997	90	30
PCM[b]	0.1-30	y = 0.6922x+ 5.2314	0.998	72	24
MFA[c]	0.1-30	y = 0.7917x+ 69.890	0.998	100	39

[a] PCM or MFA present separately in 0.1 M NaOH solution.
[b] PCM in the presence of 20 μg mL^{-1} MFA.
[c] MFA in the presence of 20 μg mL^{-1} PCM.

3.4. Effect of drugs concentration and Calibration data

The calibration curves for PCM and MFA in individual and mixture solutions (Table 1) were obtained by cyclic voltammetry measurements under the optimum experimental conditions in the concentration range of 0.1-30 μg mL^{-1} (Fig. 6). The analysis was performed on three different days by two analysts which each concentration was analyzed three times. The best calibration curves in the studied concentration range obtained were shown in Fig. 6, insets. The characteristics of the best calibration curves of PCM and MFA in 0.1 M NaOH are presented in Table 1. The investigations showed that these linear ranges were kept in mixture solutions of PCM and MFA, revealing high efficiency of the NiONPs/Gr/CPE for determinations in mixtures pharmaceutical samples of these drugs. The analytical method was validated according to the International Council for Harmonization (ICH) guidelines [39] under the optimized experimental conditions. Repeatability (intra-day) of the method was tested with each three cyclic voltammograms of three samples solutions containing lower, middle, and higher concentrations in the linear range. The intermediate precision (inter-day) of the method was evaluated by considering lower, middle and higher concentrations in linear range in three days. Values of the relative standard deviations and errors (RSD and RE %) are presented in Table 2. The results represent satisfactory precisions for the determinations of PCM and MFA in individual and mixture solutions using the NiONPs/Gr/CPE.

The accuracy of the proposed method was also studied by recovery experiments and determination of the amount of PCM in tablet and MFA in capsules at levels of 80-120% target concentration (Table 3).

Table 2. Precision and accuracy data (Intra- and inter-day).

Concentrations (μg mL^{-1})		Intra-day (n=3)			Inter-day (n=9)		
		Mean response ± SD μA	RSD (%)	RE%	Mean response ± SD μA	RSD (%)	RE%
PCM[a]	0.1	12.94 ± 0.16	1.28	-1.11	12.78 ± 0.05	0.41	5.96
	5	20.24 ± 0.06	0.33	-4.13	20.21 ± 0.13	0.65	-4.38
	30	56.66 ± 0.44	0.78	-1.85	56.22 ± 0.53	0.94	-0.46
MFA[a]	0.1	63.20 ± 1.3	2.05	1.54	63.55 ± 0.64	1.0061	3.475
	5	76.81 ± 2.45	3.20	0.01	76.76 ± 0.09	0.1221	3.164
	30	147.77 ± 1.31	1.27	-1.04	147.89 ± 0.27	0.188	-1.246
PCM[b]	0.1	5.29 ± 0.30	5.71	6.92	5.29 ± 0.01	0.052	8.006
	5	8.56 ± 0.31	3.66	0.70	8.79 ± 0.24	2.7797	-2.756
	30	28.28 ± 0.33	1.16	0.32	27.61 ± 1.25	4.53	-7.798
PCM[c]	0.1	69.99 ± 0.93	1.33	7.04	69.98 ± 0.01	0.0208	-9.482
	5	73.62 ± 0.61	0.83	0.702	73.79 ± 0.34	0.469	1.718
	30	93.69 ± 0.93	0.99	-0.03	93.60 ± 0.28	0.299	0.127

[a] PCM or MFA present separately in 0.1 M NaOH solution.
[b] PCM in the presence of 20 μg mL^{-1} MFA.
[c] MFA in the presence of 20 μg mL^{-1} PCM.

Table 3. Recovery data.

Nominal concentrations (μg mL^{-1})		standard added %	Standard added concentration (μg mL^{-1})		Recovery %	RSD %
PCM tablets	MFA capsules		PCM	MFA		
10	-	80	18	-	101.23	3.93
		100	20	-	104.91	0.70
		120	22	-	102.81	0.97
-	10	80	-	18	101.31	3.63
		100	-	20	103.37	1.58
		120	-	22	104.53	3.09
10	20	80	18	-	100.40	4.73
		100	20	-	101.83	2.20
		120	22	-	103.23	1.76
20	10	80	-	18	99.81	8.29
		100	-	20	98.55	3.30
		120	-	22	99.96	6.16

The observed recovery percent and RSD% values were shown the method is reliable for the determination of these drugs in pharmaceutical dosage form individually and combined formulations.

3.5. Analytical applications

To assess the applicability of the proposed method, the NiONPs/Gr/CPE was used to determine the content of PCM and MFA in individual related dosage

Table 4. Assay results of PCM and MFA in finished products.

Real samples		Response (n=3), μA	Mean response ± SD, μA	Obtained concentration μg mL^{-1}	RSD%	Assay%
PCM tablets (10 μg mL^{-1})		27.6				
		27.1	27.1 ± 0.42	10.06	1.55	100.60
		26.8				
MFA capsules (10 μg mL^{-1})		93.11				
		92.65	91.46 ± 2.46	10.11	2.69	101.18
		88.63				
Mixture of MFA capsules and PCM tablets (10 μg mL^{-1})		13.232				
	PCM	11.941	12.14 ± 0.99	9.84	8.23	98.43
		11.262				
		78.669				
	MFA	77.561	78.42 ± 0.75	10.02	0.96	100.21
		77.239				

Table 5. Comparison of the electrochemical behavior of NiONPs/Gr/CPE electrode for simultaneous determination PCM and MFA with some of the previously reported electrodes.

references	Calibration range (μM)		LOD (μM)		Modified electrodes
	PCM	MFA	PCM	MFA	
[40]	1–145	4–200	1	4	Glassy Carbon Electrode Modified with Multiwalled Carbon Nanotube/Chitosan Composite
[41]	0.25–900	0.3–100	0.1	0.4	copper(II) doped zeolite modified carbon paste electrode
[42]	0.5–360	2–500	0.1	0.4	1-Hexyl-3-Methylimidazolium Tetrafluoroborate/Multi-Walled Carbon Nanotube/Chitosan Nanocomposite
[43]	1–400	2–650	0.5	1	Room Temperature Ionic Liquid/Multiwalled Carbon Nanotube/Chitosan-Modified Glassy Carbon Electrode
Proposed method	0.66 – 198	0.4–120	0.12	0.13	Nickel oxide nanoparticles/ Graphene modified carbon paste electrode

forms as well as in mixture powder of PCM tablets and MFA capsules. Providing solutions with concentrations listed in Table 4, three times analyzed and the information was obtained. According to Table 4, the average value obtained at the three times acceptable analysis with RSD in the range of 0.96-9.45%. The result of the assays (n=3) undertaken yielded 100.60%, 101.18%, 98.43% and 100.21% of label claim for PCM, MFA, PCM in presence of MFA, and MFA in presence of PCM, respectively. These results of the assay indicate that the method is selective for the analysis of both PCM and MFA without interference from the excipients used to formulate and produce these products. Considering the results of the validation analysis, voltammetric method using NiONPs/Gr/CPE was found as a very sensitive method with sub-micromolar detection limits and high precision for the determinations of PCM and MFA, individually and simultaneously, in a wide concentration range in real samples. A comparison between the analytical characteristics of the present method and some previous reports for the determination of PCM and MFA is shown in Table 5.

4. Conclusions

The proposed methodology provided a new, sensitive, selective electrochemical sensor utilizing unique

properties of NiONPs and Gr such as high specific surface area, electrocatalytic and adsorptive properties. NiONPs and Gr modified CPE resulted in catalytic effects toward the electro-oxidation of PCM and MFA since it enhances the oxidation peak currents and lowers the oxidation overpotential. Therefore, simple and applicable electrochemical sensor allowed the successful determination of PCM and MFA in pharmaceutical preparations and proved that this method can be a good alternative and advantageous over the reported methods.

Acknowledgement

The financial support provided by the Tehran University of Medical Sciences Research Affairs is gratefully acknowledged.

References

[1] M.J. O'Neil, *The Merck index: an encyclopedia of chemicals, drugs, and biologicals*, RSC Publishing, **2013**.
[2] A. Brayfield, *Martindale: the complete drug reference*, 38 ed., Pharmaceutical Press, USA, **2014**.
[3] J.P. Remington, D.B. Troy and P. Beringer, *Remington: The science and practice of pharmacy*, Pharmaceutical Press, United Kingdom, **2012**.
[4] E. Dinç, C. Yücesoy and F. Onur, *J. Pharm. Biomed. Anal.*, **2002**, *28(6)*, 1091-1100.
[5] S. Das, S.C. Sharma, S.K. Talwar and P. Sethi, *Analyst*, **1989**, *114(1)*, 101-103.
[6] M.I. Toral, P. Richter, E. Araya and S. Fuentes, *Anal. Lett.*, **1996**, *29(15)*, 2679-2689.
[7] P. Parimoo, A. Bharathi and K. Padma, *Indian Drugs*, **1996**, *33(6)*, 290-292.
[8] A. Dhake, D. Sonaje, V. Kasture, P. Nikam and R. Talekar, *Indian J. Pharm. Sci.*, **2001**, *63*, 55-57.
[9] A.M. Karnik, V.P. Choudhari, S. Sharma, S. Murkute and V. Patole, *J Pharm Res Clin Pract*, **2012**, *2(2)*, 43-48.
[10] S. Husain, M. Kifayatullah and R. Sekar, *Indian J. Chem. Technol.*, **2001**, *8*, 191-194.
[11] T. Madrakian, A. Afkhami and M. Mohammadnejad, *Anal. Chim. Acta*, **2009**, *645(1)*, 25-29.
[12] S. Lokhande, S. Mhetre, S. Pekamwar and T. Kalyankar, *World Journal of Pharmacy and Pharmaceutical Sciences*, **2012**, *1*, 968-980.
[13] M.A. Badgujar and K. Mangaonkar, *J. Chem. Pharm. Res*, **2011**, *3(4)*, 893-898.
[14] A. Argekar and J. Sawant, *JPC. Journal of planar chromatography, modern TLC*, **1999**, *12(5)*, 361-364.
[15] A.B. Moghaddam, A. Mohammadi, S. Mohammadi, D. Rayeji, R. Dinarvand, M. Baghi and R.B. Walker, *Microchim. Acta*, **2010**, *171(3-4)*, 377-384.
[16] F. Ghorbani-Bidkorbeh, S. Shahrokhian, A. Mohammadi and R. Dinarvand, *J. Electroanal. Chem.*, **2010**, *638(2)*, 212-217.
[17] R. Westervelt, *Science*, **2008**, *320(5874)*, 324-325.
[18] S. Benítez–Martínez, Á.I. López-Lorente and M. Valcárcel, *Microchem. J.*, **2015**, *121*, 6-13.
[19] J. Mo, L. Zhou, X. Li, Q. Li, L. Wang and Z. Wang, *Microchem. J.*, **2017**, *130*, 353-359.
[20] J. Wang, *Electroanalysis*, **2005**, *17(1)*, 7-14.
[21] K.C.M.S. Lima, A.C.F. Santos, R.N. Fernandes, F.S. Damos and R.d.C.S. Luz, *Microchem. J.*, **2016**, *128*, 226-234.
[22] S.-J. Li, J.-Z. He, M.-J. Zhang, R.-X. Zhang, X.-L. Lv, S.-H. Li and H. Pang, *Electrochim. Acta*, **2013**, *102*, 58-65.
[23] G.-T. Liu, H.-F. Chen, G.-M. Lin, P.-p. Ye, X.-P. Wang, Y.-Z. Jiao, X.-Y. Guo, Y. Wen and H.-F. Yang, *Biosens. Bioelectron.*, **2014**, *56*, 26-32.
[24] Y.H. Ng, I.V. Lightcap, K. Goodwin, M. Matsumura and P.V. Kamat, *The Journal of Physical Chemistry Letters*, **2010**, *1(15)*, 2222-2227.
[25] A. Mohammadi, A.B. Moghaddam and J. Badraghi, *Anal. Methods*, **2012**, *4(4)*, 1024-1028.
[26] A. Mohammadi, A.B. Moghaddam, M. Kazemzad, R. Dinarvand and J. Badraghi, *Materials Science and Engineering: C*, **2009**, *29(5)*, 1752-1758.
[27] D. Gosser, *VCH, New York*, **1994**,
[28] J.B. Allen and R.F. Larry, *Electrochemical methods: fundamentals and applications*, John Wiley & Sons, Inc, New York, United States, **2001**.
[29] A. Patterson, *Phys. Rev.*, **1939**, *56(10)*, 978.
[30] H.P. Klug and L.E. Alexander, *X-ray diffraction procedures*, John Wiley and Sons, New York, United States, **1988**.
[31] F. Hahn, B. Beden, M. Croissant and C. Lamy, *Electrochim. Acta*, **1986**, *31(3)*, 335-342.
[32] P. Parpot, S. Pires and A. Bettencourt, *J. Electroanal. Chem.*, **2004**, *566(2)*, 401-408.
[33] S. Maximovitch and G. Bronoel, *Electrochim. Acta*, **1981**, *26(9)*, 1331-1338.
[34] Y. Zhang, Y. Wang, J. Jia and J. Wang, *Sensors and Actuators B: Chemical*, **2012**, *171*, 580-587.
[35] A. Feizbakhsh, A. Aghassi, A. Ehsani, M.A. Jamaat, A. Naeemy and I. Danaee, *J. Chin. Chem. Soc.*, **2012**, *59(9)*, 1086-1093.
[36] I. Casella, E. Desimoni and T. Cataldi, *Anal. Chim. Acta*, **1991**, *248(1)*, 117-125.
[37] M. Fleischmann, K. Korinek and D. Pletcher, *J. Electroanal. Chem.* **1971**, *31(1)*, 39-49.
[38] J. Losada, I. Del Peso and L. Beyer, *J. Electroanal. Chem.*, **1998**, *447(1)*, 147-154.
[39] ICH, *Validation of analytical procedures: text and methodology (Q2R1)*, International Conference on Harmonization, Geneva: IFPMA, **2005**.
[40] A. Babaei, M. Afrasiabi and M. Babazadeh,

Electroanalysis, **2010**, *22(15)*, 1743-1749.
[41] B. Khalilzadeh, A. Babaei and M. Afrasiabi, *J. Appl. Electrochem.*, **2010**, *40(8)*, 1537-1543.
[42] A. Asghari, S. Kianipour, M. Afrasiabi and M. Rajabi, *Sensor Letters*, **2013**, *11(3)*, 545-551.
[43] S. Kianipour and A. Asghari, *Sensors Journal, IEEE*, **2013**, *13(7)*, 2690-2698.